Exact Solution for Rectangular Sandwich Plates with Embedded Piezoelectric Shear Actuators

Senthil S. Vel*
University of Maine, Orono, Maine 04469
and
R. C. Batra[†]
Virginia Polytechnic Institute and State University, Blacksburg, Virginia 24061

An exact solution is obtained for the three-dimensional deformations of simply supported laminated rectangular thick plates with embedded shear mode piezoelectric actuators, subjected to mechanical and electrical loading on the upper and lower surfaces. Each layer of the laminate is made of either an orthotropic elastic material or a piezoelectric material whose poling direction lies in the plane of the plate, with perfect bonding between the adjoining layers. The exact displacements and stresses for a homogeneous piezoelectric plate for various length-to-thickness ratios are compared with those obtained by the first-order shear deformation theory. Results are also presented for a sandwich plate consisting of a shear mode piezoelectric core sandwiched between two elastic layers. A comparison of the stresses with those in the corresponding surface-mounted extension actuation configuration shows that for the same transverse deflection of the plate centroid, the maximum longitudinal stress within the actuator is significantly smaller for the shear actuation mechanism. The exact results presented here can be used to assess the accuracy of different plate theories and/or for validating finite element codes.

I. Introduction

IN recent years, piezoelectric materials have been integrated with structural systems to form a class of smart structures. The piezoelectric materials are capable of altering the structure's response through sensing and actuation. By the integration of surface-bonded and embedded actuators into structural systems, desired localized strains may be induced in the structure by the application of an appropriate voltage to the actuators.

A piezoelectric actuator in an adaptive structure is a thin rectangular element that is generally poled in the thickness direction and is usually bonded to the surfaces of the host structure. The application of an electric field in the thickness direction causes the actuator's lateral dimensions to increase or decrease. The lateral deformations of the actuator force the host structure to deform. Such surface-bonded actuators, which induce longitudinal strains by extension or contraction, are known as extension actuators. To incorporate actuators into a structure successfully the mechanical interaction between the actuators and the host structure must be fully understood. Mechanical models for extension actuators have been developed by Crawley and de Luis,[1] Crawley and Anderson,[2] and others for piezoelectric patches bonded to a beam. Lee,[3] Huang and Wu,[4] Mitchell and Reddy,[5] and others have developed plate theories for rectangular hybrid laminates. Numerous finite element analyses have also been conducted, for example, see Robbins and Reddy[6] and Batra and Liang.[7] Ray et al.[8] and Heyliger and Brooks[9] have obtained exact three-dimensional solutions for the cylindrical bending of simply supported piezoelectric laminates. Exact solutions for simply supported rectangular piezoelectric laminates were given by Heyliger,[10,11] Bisegna and Maceri,[12] and Lee and Jiang.[13] A similar technique was employed by Yang et al.[14] and Batra et al.[15] to analyze the vibrations of a simply supported plate with piezoceramic actuators either bonded to its upper and lower surfaces or embedded within the laminate. Vel and Batra[16,17] have derived three-dimensional analytical solutions for thick piezo-electric plates subjected to arbitrary boundary conditions at the edges.

Extension piezoelectric actuators are usually placed at the extreme thickness positions of a platelike structure to achieve the most effective actuation. This subjects the actuators to high longitudinal stresses that may be detrimental to the brittle piezoceramic material. Furthermore, surface-bonded actuators are likely to be damaged by contact with surrounding objects. To alleviate these problems, Sun and Zhang[18] proposed an adaptive sandwich structure consisting of an axially poled piezoelectric core sandwiched between two elastic facing sheets. The application of an electric field in the thickness direction would induce transverse shear deformation of the core, thus generating the desired transverse deflection of the sandwich structure. Piezoelectric actuators poled in such a way as to produce transverse shear deformation under the action of an electric field in the thickness direction are called shear actuators. Piezoelectric shear actuators of various dimensions are commercially available.[19] Zhang and Sun[20,21] developed a beam theory for sandwich structures containing shear actuators by modeling the facing sheets as classical Euler–Bernoulli beams and the central core as a Timoshenko beam, which allows transverse shear deformation. They state that it is very difficult to find a general solution for the fully coupled electromechanical equations of a sandwich beam. Benjeddou et al.[22] developed a unified finite element model for extension and shear actuation mechanisms with more detailed formulation of the electric problem. Vidoli and Batra[23] have developed a plate theory for an anisotropic piezoelectric plate that accounts for changes in the thickness of the plate caused by the double forces without moments applied to the top and bottom surfaces of the plate, as well as both shear and extension actuation effects. They exhibited the relative importance of these effects by studying the deformations of a beam with the poling axis, not necessarily along the thickness direction. The electric field was applied in the thickness direction. Vel and Batra[24] used the Eshelby–Stroh formalism to obtain analytical solutions for a piezoelectric bimorph. The axis of transverse isotropy in each layer of the bimorph was assumed not necessarily to be perpendicular to the midsurface of the layer.

The exact solutions for piezoelectric extension actuators given by Heyliger,[10,11] Bisegna and Maceri,[12] and Lee and Jiang[13] are not applicable to piezoelectric shear actuators because they assume that the only nonzero components of the piezoelectric tensor e_{ijk} in the contracted notation [see Eq. (2)] are $e_{31}, e_{32}, e_{33}, e_{24}$, and e_{15}. For
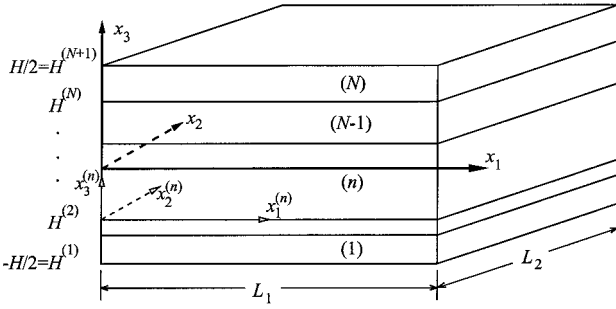
Fig. 1   N-layer laminated piezoelectric plate.

a piezoelectric shear actuator poled in the x_1 direction (Fig. 1), the nonzero components of the piezoelectric tensor in the contracted notation are $e_{11}, e_{12}, e_{13}, e_{26}$, and e_{35}. Recently, Vel and Batra[25] gave an exact solution for the cylindrical bending of a simply supported sandwich plate with a piezoelectric shear actuator, wherein the plate was assumed to be infinitely long in the x_2 direction. Here, we extend the method to simply supported rectangular plates of finite dimensions with embedded piezoelectric shear actuators. The three-dimensional governing equations of linear piezoelectricity are exactly satisfied at every point in the laminate. The boundary conditions at the simply supported edges, the traction boundary conditions on the top and bottom surfaces, and the electromechanical continuity conditions at the interfaces between dissimilar layers are also exactly satisfied. The electrical boundary conditions at two opposite grounded edges and at the other two electrically insulated edges are also exactly satisfied. The displacements and stresses for a homogeneous piezoelectric plate are compared with those obtained from the first-order shear deformation theory (FSDT). Sandwich plates with a shear mode piezoelectric core sandwiched between two elastic layers are also studied. When the results are compared with those for the corresponding structure with surface-mounted extension actuators, it is seen that the maximum longitudinal stress within the shear actuator is significantly lower than that in the extension actuator for the same transverse deflection of the plate.

Results presented herein should be useful for validating and, if necessary, refining simpler models of the system.

II.   Formulation of the Problem

We use a rectangular Cartesian coordinate system, shown in Fig. 1, to describe the infinitesimal quasi-static deformations of an N-layer piezoelectric laminated rectangular plate occupying the region $[0, L_1] \times [0, L_2] \times [H^{(1)}, H^{(N+1)}]$ in the unstressed reference configuration. The vertical positions of the bottom and top surfaces as well as of the $N - 1$ interfaces between the adjoining laminas are denoted by $H^{(1)} = -H/2$, $H^{(2)}, \ldots, H^{(n)}$, $\ldots, H^{(N)}, H^{(N+1)} = H/2$. Each lamina is assumed to be made of a homogeneous material.

The equilibrium equations for the nth lamina made of a piezoelectric material, in the absence of body forces and free charges, are

$$\sigma_{ij,j}^{(n)} = 0, \qquad D_{j,j}^{(n)} = 0 \qquad (i, j = 1, 2, 3) \qquad (1)$$

where σ_{ij} are the components of the Cauchy stress tensor and D_j the electric displacement. A comma followed by index j indicates partial differentiation with respect to the present position x_j of a material particle, a repeated index implies summation over the range of the index, and the superscript (n) signifies quantities for the nth lamina.

The elastic layers are orthotropic with planes of symmetry coincident with the coordinate planes. The piezoelectric material is modeled as transversely isotropic, with the x_1 axis as the axis of transverse isotropy, which is also the poling direction. The constitutive equations, in contracted notation, for the nth lamina are

$$\begin{Bmatrix} \sigma_{11} \\ \sigma_{22} \\ \sigma_{33} \\ \sigma_{32} \\ \sigma_{31} \\ \sigma_{12} \end{Bmatrix}^{(n)} = \begin{bmatrix} C_{11} & C_{12} & C_{13} & 0 & 0 & 0 \\ C_{12} & C_{22} & C_{23} & 0 & 0 & 0 \\ C_{13} & C_{23} & C_{33} & 0 & 0 & 0 \\ 0 & 0 & 0 & C_{44} & 0 & 0 \\ 0 & 0 & 0 & 0 & C_{55} & 0 \\ 0 & 0 & 0 & 0 & 0 & C_{66} \end{bmatrix}^{(n)} \begin{Bmatrix} \varepsilon_{11} \\ \varepsilon_{22} \\ \varepsilon_{33} \\ 2\varepsilon_{23} \\ 2\varepsilon_{31} \\ 2\varepsilon_{12} \end{Bmatrix}^{(n)}$$

$$- \begin{bmatrix} e_{11} & 0 & 0 \\ e_{12} & 0 & 0 \\ e_{13} & 0 & 0 \\ 0 & 0 & 0 \\ 0 & 0 & e_{35} \\ 0 & e_{26} & 0 \end{bmatrix}^{(n)} \begin{Bmatrix} E_1 \\ E_2 \\ E_3 \end{Bmatrix}^{(n)}$$

$$\begin{Bmatrix} D_1 \\ D_2 \\ D_3 \end{Bmatrix}^{(n)} = \begin{bmatrix} e_{11} & e_{12} & e_{13} & 0 & 0 & 0 \\ 0 & 0 & 0 & 0 & 0 & e_{26} \\ 0 & 0 & 0 & 0 & e_{35} & 0 \end{bmatrix}^{(n)} \begin{Bmatrix} \varepsilon_{11} \\ \varepsilon_{22} \\ \varepsilon_{33} \\ 2\varepsilon_{23} \\ 2\varepsilon_{31} \\ 2\varepsilon_{12} \end{Bmatrix}^{(n)}$$

$$+ \begin{bmatrix} \epsilon_{11} & 0 & 0 \\ 0 & \epsilon_{22} & 0 \\ 0 & 0 & \epsilon_{33} \end{bmatrix}^{(n)} \begin{Bmatrix} E_1 \\ E_2 \\ E_3 \end{Bmatrix}^{(n)} \qquad (2)$$

where ε_{ij} are the components of the infinitesimal strain tensor, E_j the electric field, C_{ij} the elasticity constants, e_{ij} the piezoelectric moduli, and ϵ_{ij} the electric permittivity. Material elasticities and permitivities are assumed to yield a positive stored energy density for every nonrigid deformation and/or nonzero electric field.[26] For an elastic layer, the piezoelectric moduli vanish identically. The number of independent elastic moduli C_{ij} equals nine for an orthotropic material and five for a transversely isotropic material. The infinitesimal strain tensor and the electric field are related to the mechanical displacements u_j and the electric potential ϕ by

$$\varepsilon_{ij}^{(n)} = \tfrac{1}{2}\left(u_{i,j}^{(n)} + u_{j,i}^{(n)}\right), \qquad E_j^{(n)} = -\phi_{,j}^{(n)} \qquad (3)$$

The edges $x_1 = 0$ and L_1 are assumed to be mechanically simply supported and electrically insulated, and the edges $x_2 = 0$ and L_2 are assumed to be mechanically simply supported and electrically grounded. That is,

$$\sigma_{11}^{(n)} = 0, \quad u_2^{(n)} = u_3^{(n)} = 0, \quad D_1^{(n)} = 0 \quad \text{at} \quad x_1 = 0, L_1$$

$$\sigma_{22}^{(n)} = 0, \quad u_1^{(n)} = u_3^{(n)} = 0, \quad \phi^{(n)} = 0 \quad \text{at} \quad x_2 = 0, L_2$$

$$(4)$$

The mechanical boundary conditions of a simply supported plate for the stresses and displacements in Eq. (4) are identical to those assumed by Heyliger[11] for the exact solution of rectangular plates with extension actuators. Exact three-dimensional solutions for laminated plates can be obtained only for certain combinations of boundary conditions on the edges. Heyliger[11] considered electrically grounded ($\phi^{(n)} = 0$) edges at $x_1 = 0, L_1$ to obtain exact solutions for laminates with piezoelectric extension actuators. In the case of piezoelectric shear actuators, we are able to obtain exact solutions only when the edges $x_1 = 0$ and L_1 are electrically insulated ($D_1^{(n)} = 0$).

The boundary conditions prescribed on the top and bottom surfaces of the laminate can be either a mechanical displacement component u_j or the corresponding traction component σ_{3j} and either the electric potential ϕ or the normal component of the electric displacement D_3. However, typically nonzero normal tractions, zero tangential tractions, and electric potential are prescribed on the top and bottom surfaces of a plate. Because the applied pressure and

electric potential can be expanded in terms of a Fourier series, it is sufficient to consider electrical and/or mechanical loads of the form

$$\phi(x_1, x_2, H/2) = \phi_0 \cos px_1 \sin qx_2$$

$$\sigma_{33}(x_1, x_2, H/2) = q_0 \sin px_1 \sin qx_2 \tag{5}$$

where ϕ_0 and q_0 are known constants, $p = k\pi/L_1$, $q = m\pi/L_2$, and k and m are nonnegative integers.

The interface conditions on the material surfaces $x_3 = H^{(2)}$, $\ldots$, $H^{(N)}$ may be specified as follows:

1) If the surface $x_3 = H^{(n+1)}$ is an interface between two laminas, the mechanical displacements, surface tractions, the electric potential, and the normal component of the electric displacement between them are continuous. That is

$$u_j^{(n)} = u_j^{(n+1)}, \qquad \sigma_{3j}^{(n)} = \sigma_{3j}^{(n+1)}, \qquad \phi^{(n)} = \phi^{(n+1)}$$

$$D_3^{(n)} = D_3^{(n+1)} \qquad \text{on} \qquad x_3 = H^{(n+1)} \tag{6}$$

Thus, the adjoining laminas are presumed to be mechanically and electrically perfectly bonded together.

2) If the interface $x_3 = H^{(n+1)}$ is electroded, then the electric potential on this surface is assumed to be a known function of the form $\phi_0^{(n+1)} \cos px_1 \sin qx_2$. The normal component of the electric displacement need not be continuous across this interface. Thus,

$$u_j^{(n)} = u_j^{(n+1)}, \qquad \sigma_{3j}^{(n)} = \sigma_{3j}^{(n+1)}$$

$$\phi^{(n)} = \phi^{(n+1)} = \phi_0^{(n+1)} \cos px_1 \sin qx_2 \qquad \text{on} \qquad x_3 = H^{(n+1)} \tag{7}$$

III. Exact Solution

We construct a local coordinate system $x_1^{(n)}$, $x_2^{(n)}$, $x_3^{(n)}$ with the local axes parallel to the global axes and the origin at the point where the global x_3 axis intersects the bottom surface of the nth lamina (see Fig. 1). In this local coordinate system, the nth lamina occupies the region $[0, L_1] \times [0, L_2] \times [0, h^{(n)}]$, where $h^{(n)} = H^{(n+1)} - H^{(n)}$. We drop the superscript n for convenience, with the understanding that all material constants and unknowns are for the nth lamina. An exact solution is obtained by extending the state-space formulation of Fan and Ye[27] to piezoelectric shear actuators.

Because the stored energy density is positive, the material constants C_{33}, C_{44}, C_{55}, and ϵ_{33} are positive quantities and $C_{55}\epsilon_{33} + e_{35}^2 > 0$. Solving for $u_{1,3}$ and $\phi_{,3}$ from the constitutive equations for σ_{31} and D_3 in Eq. (2), we obtain

$$u_{1,3} = \frac{\epsilon_{33}}{(C_{55}\epsilon_{33} + e_{35}^2)}\sigma_{31} + \frac{e_{35}}{(C_{55}\epsilon_{33} + e_{35}^2)}D_3 - u_{3,1}$$

$$\phi_{,3} = \frac{e_{35}}{(C_{55}\epsilon_{33} + e_{35}^2)}\sigma_{31} - \frac{C_{55}}{(C_{55}\epsilon_{33} + e_{35}^2)}D_3 \tag{8}$$

From the constitutive equations for σ_{32} and σ_{33} in Eq. (2), we have

$$u_{2,3} = \frac{1}{C_{44}}\sigma_{32} - u_{3,2}$$

$$u_{3,3} = \frac{1}{C_{33}}\sigma_{33} - \frac{C_{13}}{C_{33}}u_{1,1} - \frac{C_{23}}{C_{33}}u_{2,2} - \frac{e_{13}}{C_{33}}\phi_{,1} \tag{9}$$

The following equations are obtained by eliminating the in-plane stresses σ_{11}, σ_{22}, and σ_{12} and the in-plane electric displacements D_1 and D_2 from the equilibrium equations (1) by using the constitutive relations (2), (8), and (9):

$$\sigma_{31,3} = -\left(C_{11} - \frac{C_{13}^2}{C_{33}}\right)u_{1,11} - C_{66}u_{1,22} - \left(C_{12} + C_{66} - \frac{C_{13}C_{23}}{C_{33}}\right)$$

$$\times u_{2,21} - \frac{C_{13}}{C_{33}}\sigma_{33,1} - \left(e_{11} - \frac{C_{13}e_{13}}{C_{33}}\right)\phi_{,11} - e_{26}\phi_{,22}$$

$$\sigma_{32,3} = -\left(C_{66} + C_{12} - \frac{C_{13}C_{23}}{C_{33}}\right)u_{1,12} - C_{66}u_{2,11} - \left(C_{22} - \frac{C_{23}^2}{C_{33}}\right)$$

$$\times u_{2,22} - \frac{C_{23}}{C_{33}}\sigma_{33,2} - \left(e_{12} + e_{26} - \frac{C_{23}e_{13}}{C_{33}}\right)\phi_{,12}$$

$$\sigma_{33,3} = -\sigma_{31,1} - \sigma_{32,2}$$

$$D_{3,3} = -\left(e_{11} - \frac{C_{13}e_{13}}{C_{33}}\right)u_{1,11} - \left(e_{12} + e_{26} - \frac{C_{23}e_{13}}{C_{33}}\right)u_{2,12}$$

$$- e_{26}u_{1,22} - \frac{e_{13}}{C_{33}}\sigma_{33,1} + \left(\epsilon_{11} + \frac{e_{13}^2}{C_{33}}\right)\phi_{,11} + \epsilon_{22}\phi_{,22} \tag{10}$$

Equations (8–10) are the state-space equations for the eight state-space variables u_1, u_2, u_3, ϕ, σ_{31}, σ_{32}, σ_{33}, and D_3 for piezoelectric materials that are poled in the x_1 direction. The state-space equations for elastic materials given by Fan and Ye[27] can be recovered by setting the piezoelectric coefficients e_{ij} to zero in the first of Eqs. (8), Eqs. (9), and the first three of Eqs. (10).

A solution to the state-space variables for the nth lamina is sought in the form

$$[u_1, \phi, \sigma_{31}, D_3] = [\bar{u}_1, \bar{\phi}, \bar{\sigma}_{31}, \bar{D}_3] \cos px_1 \sin qx_2$$

$$[u_2, \sigma_{32}] = [\bar{u}_2, \bar{\sigma}_{32}] \sin px_1 \cos qx_2$$

$$[u_3, \sigma_{33}] = [\bar{u}_3, \bar{\sigma}_{33}] \sin px_1 \sin qx_2 \tag{11}$$

Equations (11) identically satisfy the homogeneous boundary conditions (4) on the edges $x_1 = 0$ and L_1 and $x_2 = 0$ and L_2. Expressions for u_1, u_2, etc., for extension actuators look similar to those given in Eq. (11), except that the trigonometric functions of x_1 and x_2 are different. Substitution for u_1, u_2, u_3, ϕ, σ_{31}, σ_{32}, σ_{33}, and D_3 from Eq. (11) into Eqs. (8–10) leads to the following matrix equation:

$$\frac{dS(x_3)}{dx_3} = AS(x_3) \tag{12}$$

where

$$S = [\bar{u}_1 \quad \bar{u}_2 \quad \bar{\sigma}_{33} \quad \bar{\phi} \quad \bar{\sigma}_{31} \quad \bar{\sigma}_{32} \quad \bar{u}_3 \quad \bar{D}_3]^T, \qquad A = \begin{bmatrix} 0 & P \\ Q & 0 \end{bmatrix}$$

$$P = \begin{bmatrix} \dfrac{\epsilon_{33}}{(C_{55}\epsilon_{33} + e_{35}^2)} & 0 & -p & \dfrac{e_{35}}{(C_{55}\epsilon_{33} + e_{35}^2)} \\ 0 & \dfrac{1}{C_{44}} & -q & 0 \\ p & q & 0 & 0 \\ \dfrac{e_{35}}{(C_{55}\epsilon_{33} + e_{35}^2)} & 0 & 0 & -\dfrac{C_{55}}{(C_{55}\epsilon_{33} + e_{35}^2)} \end{bmatrix}$$

$$Q = \begin{bmatrix} p^2\left(C_{11} - \dfrac{C_{13}^2}{C_{33}}\right) + q^2 C_{66} & pq\left(C_{12} + C_{66} - \dfrac{C_{13}C_{23}}{C_{33}}\right) & -p\dfrac{C_{13}}{C_{33}} & p^2\left(e_{11} - \dfrac{C_{13}e_{13}}{C_{33}}\right) + q^2 e_{26} \\ pq\left(C_{12} + C_{66} - \dfrac{C_{13}C_{23}}{C_{33}}\right) & p^2 C_{66} + q^2\left(C_{22} - \dfrac{C_{23}^2}{C_{33}}\right) & -q\dfrac{C_{23}}{C_{33}} & pq\left(e_{12} + e_{26} - \dfrac{C_{23}e_{13}}{C_{33}}\right) \\ p\dfrac{C_{13}}{C_{33}} & q\dfrac{C_{23}}{C_{33}} & \dfrac{1}{C_{33}} & p\dfrac{e_{13}}{C_{33}} \\ p^2\left(e_{11} - \dfrac{C_{13}e_{13}}{C_{33}}\right) + q^2 e_{26} & pq\left(e_{12} + e_{26} - \dfrac{C_{23}e_{13}}{C_{33}}\right) & -p\dfrac{e_{13}}{C_{33}} & -p^2\left(\epsilon_{11} + \dfrac{e_{13}^2}{C_{33}}\right) - q^2\epsilon_{22} \end{bmatrix}$$

Integration of the vector differential equation (12) gives

$$S(x_3) = \exp[x_3 A]Z \tag{13}$$

where Z is an 8×1 vector of unknown coefficients. To evaluate the matrix exponential in Eq. (13) explicitly, we expand it into a matrix polynomial as

$$\exp[x_3 A] = \sum_{j=1}^{8} \alpha_j(x_3) A^{j-1} \tag{14}$$

where no powers of A higher than seven are needed due to the Cayley–Hamilton theorem. In terms of the matrices P and Q, the matrix exponential is

$$\exp[x_3 A] = \begin{bmatrix} \alpha_1(x_3)\mathbf{1} + \alpha_3(x_3)PQ + \alpha_5(x_3)PQPQ & \alpha_2(x_3)P + \alpha_4(x_3)PQP \\ +\alpha_7(x_3)PQPQPQ & +\alpha_6(x_3)PQPQP + \alpha_8(x_3)PQPQPQP \\ \alpha_2(x_3)Q + \alpha_4(x_3)QPQ & \alpha_1(x_3)\mathbf{1} + \alpha_3(x_3)QP + \alpha_5(x_3)QPQP \\ +\alpha_6(x_3)QPQPQ + \alpha_8(x_3)QPQPQPQ & +\alpha_7(x_3)QPQPQP \end{bmatrix}$$

The coefficients $\alpha_j(x_3)$ are determined in terms of the eigenvalues λ of matrix A by the observation that they satisfy the characteristic equation

$$\exp[x_3 \lambda] = \sum_{j=1}^{8} \alpha_j(x_3) \lambda^{j-1} \tag{15}$$

If the eigenvalues are distinct, using Eq. (15) eight times, once for each eigenvalue λ_j, $j = 1, \ldots, 8$, generates an algebraic system of equations in the eight unknowns $\alpha_j(x_3)$ whose solution is

$$\begin{bmatrix} \alpha_1(x_3) \\ \alpha_2(x_3) \\ \vdots \\ \alpha_8(x_3) \end{bmatrix} = \begin{bmatrix} 1 & \lambda_1 & \lambda_1^2 & \cdots & \lambda_1^7 \\ 1 & \lambda_2 & \lambda_2^2 & \cdots & \lambda_2^7 \\ \vdots & \vdots & \vdots & & \vdots \\ 1 & \lambda_8 & \lambda_8^2 & \cdots & \lambda_8^7 \end{bmatrix}^{-1} \begin{bmatrix} e^{\lambda_1 x_3} \\ e^{\lambda_2 x_3} \\ \vdots \\ e^{\lambda_8 x_3} \end{bmatrix} \tag{16}$$

Alternatively, the matrix exponential in Eq. (13) can be evaluated by using the Jordan decomposition of matrix A. Any square matrix A can be decomposed as

$$A = TJT^{-1} \tag{17}$$

where J is the Jordan canonical form of A and T is a similarity matrix. The matrix J is usually a diagonal matrix of eigenvalues of A, but, in general, it could also have ones directly above the diagonal if the eigenvalues are repeated. The matrix exponential can then be evaluated as

$$\exp[x_3 A] = T \exp[x_3 J] T^{-1} \tag{18}$$

where the matrix exponential $\exp[x_3 J]$ may be written down by inspection of the Jordan matrix J.

On evaluating the matrix exponential, we obtain analytical expressions for the state-space variables $u_1, u_2, u_3, \phi, \sigma_{31}, \sigma_{32}, \sigma_{33}$, and D_3 of each lamina in terms of eight scalar coefficients Z_j. The coefficients are determined by satisfying the boundary conditions on the top and bottom surfaces of the laminate as well as the interface conditions (6) or (7) between adjoining dissimilar plies. This results in four conditions on both the top and bottom surfaces and eight conditions at each of the $N-1$ interfaces. The resulting system of $8N$ linear algebraic equations for the $8N$ unknowns $Z_j^{(n)}$ ($n = 1, 2, \ldots, N$) is readily solved. After the constants are determined, the mechanical displacements, stresses, electric potential, and electric displacement can be computed at any location within the laminate.

IV. FSDT Solution

In this section we develop an analytical solution for the deformations of a transversely isotropic homogeneous rectangular piezoelectric plate by using the FSDT plate theory. Assume that the plate is of thickness H, that it is poled in the x_1 direction, that its edges are simply supported, that the edges $x_1 = 0$ and L_1 are electrically insulated and the edges $x_2 = 0$ and L_2 are electrically grounded, and that the top and bottom surfaces are subjected to the following electric and/or mechanical loads:

$$\phi(x_1, x_2, \pm H/2) = \pm \phi_0 \cos(\pi x_1/L_1) \sin(\pi x_2/L_2)$$

$$\sigma_{3j}(x_1, x_2, H/2) = q_0 \delta_{3j} \sin(\pi x_1/L_1) \sin(\pi x_2/L_2) \tag{19}$$

where ϕ_0 and q_0 are known constants and δ_{3j} is the Kronecker delta. We take the midsurface of the plate as the reference surface and assume the following fields, based on the FSDT, for the displacements and the electric potential:

$$u_i(x_1, x_2, x_3) = u_i^0(x_1, x_2) + x_3(1 - \delta_{3i})\varphi_i(x_1, x_2) \quad \text{(no sum on } i\text{)}$$

$$\phi(x_1, x_2, x_3) = 2\phi_0(x_3/H) \cos(\pi x_1/L_1) \sin(\pi x_2/L_2) \tag{20}$$

Here $u_i^0(x_1, x_2)$ are the displacements of a point on the midsurface, and $\varphi_1(x_1, x_2)$ and $-\varphi_2(x_1, x_2)$ are the rotations of the normal to the midsurface about the x_2 and x_1 axes, respectively. The nonzero infinitesimal strains and the components of the electric field associated with Eq. (20) are

$$\varepsilon_{11} = u_{1,1}^0 + x_3 \varphi_{1,1}, \qquad \varepsilon_{22} = u_{2,2}^0 + x_3 \varphi_{2,2}, \qquad 2\varepsilon_{23} = u_{3,2}^0 + \varphi_2$$

$$2\varepsilon_{13} = u_{3,1}^0 + \varphi_1, \qquad 2\varepsilon_{12} = \left(u_{1,2}^0 + u_{2,1}^0\right) + x_3(\varphi_{1,2} + \varphi_{2,1})$$

$$E_1 = 2\phi_0(\pi x_3/HL_1) \sin(\pi x_1/L_1) \sin(\pi x_2/L_2)$$

$$E_2 = -2\phi_0(\pi x_3/HL_2) \cos(\pi x_1/L_1) \cos(\pi x_2/L_2)$$

$$E_3 = -2(\phi_0/H) \cos(\pi x_1/L_1) \sin(\pi x_2/L_2) \tag{21}$$

The reduced stress–strain relationship (22) is obtained by setting $\sigma_{33} = 0$ in Eq. (2). From this assumption, ε_{33} is computed in terms of $\varepsilon_{11}, \varepsilon_{22}$, and E_1 and then substituted into the expressions for $\sigma_{11}, \sigma_{22}, \sigma_{23}, \sigma_{13}$, and σ_{12} in Eq. (2). A limitation of the FSDT is that both σ_{33} and ε_{33} are assumed to vanish; this has been corrected in the plate theory proposed by Vidoli and Batra.[23] In the FSDT the through-thickness variation of σ_{33} is computed by the integration of the equilibrium equations in the thickness direction.

$$\begin{Bmatrix} \sigma_{11} \\ \sigma_{22} \\ \sigma_{23} \\ \sigma_{13} \\ \sigma_{12} \end{Bmatrix} = \begin{bmatrix} Q_{11} & Q_{12} & 0 & 0 & 0 & -P_{11} & 0 & 0 \\ Q_{12} & Q_{22} & 0 & 0 & 0 & -P_{12} & 0 & 0 \\ 0 & 0 & Q_{44} & 0 & 0 & 0 & 0 & 0 \\ 0 & 0 & 0 & Q_{55} & 0 & 0 & 0 & -P_{35} \\ 0 & 0 & 0 & 0 & Q_{66} & 0 & -P_{26} & 0 \end{bmatrix} \begin{Bmatrix} \varepsilon_{11} \\ \varepsilon_{22} \\ 2\varepsilon_{23} \\ 2\varepsilon_{13} \\ 2\varepsilon_{12} \\ E_1 \\ E_2 \\ E_3 \end{Bmatrix} \tag{22}$$

where

$$Q_{11} = C_{11} - \left(C_{13}^2/C_{33}\right), \qquad Q_{12} = C_{12} - (C_{13}C_{23}/C_{33})$$

$$Q_{22} = C_{22} - \left(C_{23}^2/C_{33}\right), \qquad Q_{44} = C_{44}, \qquad Q_{55} = C_{55}$$

$$Q_{66} = C_{66}, \qquad P_{11} = e_{11} - C_{13}e_{13}/C_{33}$$

$$P_{12} = e_{12} - C_{23}e_{13}/C_{33}, \qquad P_{35} = e_{35}, \qquad P_{26} = e_{26} \quad (23)$$

The variational principle for a simply supported piezoelectric plate (for example, see Tiersten[26]) gives the governing equations

$$N_{11,1} + N_{12,2} = 0, \qquad M_{11,1} + M_{12,2} - Q_1 = 0$$

$$N_{22,2} + N_{12,1} = 0, \qquad M_{22,2} + M_{12,1} - Q_2 = 0$$

$$Q_{1,1} + Q_{2,2} + q_0 \sin(\pi x_1/L_1) \sin(\pi x_2/L_2) = 0 \quad (24)$$

and boundary conditions

$$N_{11} = 0, \qquad M_{11} = 0, \qquad u_2^0 = 0, \qquad \varphi_2 = 0, \qquad u_3^0 = 0$$

$$D_1 = 0 \quad \text{at} \quad x_1 = 0 \quad \text{and} \quad L_1$$

$$N_{22} = 0, \qquad M_{22} = 0, \qquad u_1^0 = 0, \qquad \varphi_1 = 0, \qquad u_3^0 = 0$$

$$\phi = 0 \quad \text{at} \quad x_2 = 0 \quad \text{and} \quad L_2 \quad (25)$$

The stress resultants are defined as

$$[N_{ij}, M_{ij}] = \int_{-H/2}^{H/2} \sigma_{ij}[1, x_3] \, dx_3, \qquad Q_i = \mathcal{K} \int_{-H/2}^{H/2} \sigma_{i3} \, dx_3 \quad (26)$$

where $\mathcal{K}$ is the shear correction factor. We note that the electrical boundary conditions in the 6th and 12th of Eqs. (25) are not given by the variational principle because the electric potential distribution is assumed a priori. The charge equation, second of Eqs. (1), has not been considered in the derivation of the equilibrium equations (24) because there is no contribution from the electric internal virtual work term $\int D_i \delta E_i$ in the variational statement.

A solution to the differential equations (24) is obtained by choosing the displacements and rotations as

$$\left[u_1^0(x_1, x_2), \varphi_1(x_1, x_2)\right] = [R_1, R_2] \cos(\pi x_1/L_1) \sin(\pi x_2/L_2)$$

$$\left[u_2^0(x_1, x_2), \varphi_2(x_1, x_2)\right] = [R_3, R_4] \sin(\pi x_1/L_1) \cos(\pi x_2/L_2)$$

$$u_3^0(x_1, x_2) = R_5 \sin(\pi x_1/L_1) \sin(\pi x_2/L_2) \quad (27)$$

These and the electric potential given by the second of Eqs. (20), satisfy edge conditions (25) identically. Substitution for u_i^0, φ_1, and φ_2 from Eq. (27) into Eq. (21) and the resulting expressions for ε_{ij} and E_i into Eq. (22) gives stresses in terms of ϕ_0 and the unknowns R_k, $k = 1, \ldots, 5$. These expressions for the stresses are then substituted into Eq. (26) and for the stress resultants into Eq. (24) to obtain five simultaneous linear equations for the five unknowns R_k, which can be readily solved. The solution for R_k when the plate is subjected only to an electric load is given in the Appendix.

V. Results and Discussion

We present results first for a homogeneous piezoelectric plate and then for sandwich structures with each lamina made of either graphite–epoxy or PZT-5A, whose nonzero material properties are listed in Table 1. The graphite–epoxy is assumed to be orthotropic, and the PZT-5A is transversely isotropic with x_1 axis as the axis of transverse isotropy, which is also the poling direction. The material properties of the axially poled PZT-5A were obtained by a tensor transformation of the material properties given by Tang et al.[28] of PZT-5A poled in the x_3 direction.

Table 1 Nonvanishing material properties of the graphite–epoxy and PZT-5A shear actuators

Property	Graphite–epoxy	Shear PZT-5A
C_{11} (GPa)	183.443	86.856
C_{22} (GPa)	11.662	99.201
C_{33} (GPa)	11.662	99.201
C_{12} (GPa)	4.363	50.778
C_{13} (GPa)	4.363	50.778
C_{23} (GPa)	3.918	54.016
C_{44} (GPa)	2.870	22.593
C_{55} (GPa)	7.170	21.100
C_{66} (GPa)	7.170	21.100
e_{11} (Cm^{-2})	0	15.118
e_{12} (Cm^{-2})	0	−7.209
e_{13} (Cm^{-2})	0	−7.209
e_{26} (Cm^{-2})	0	12.322
e_{35} (Cm^{-2})	0	12.322
ϵ_{11} (10^{-10} F/m)	153.0	150.0
ϵ_{22} (10^{-10} F/m)	153.0	153.0
ϵ_{33} (10^{-10} F/m)	153.0	153.0

A. Homogeneous Piezoelectric Plate

Consider a homogeneous square plate made of the piezoceramic PZT-5A and subjected to the sinusoidal electric and/or mechanical loads (19) on the top and bottom surfaces. The mechanical displacements, stresses, electric displacements, and electric potential are nondimensionalized as

$$\hat{u}_i = u_i C_0/e_0\phi_0, \qquad \hat{\sigma}_{ij} = \sigma_{ij}L_1/e_0\phi_0$$

$$\hat{D}_i = D_i L_1 C_0 \big/ e_0^2\phi_0, \qquad \hat{\phi} = \phi/\phi_0$$

for the applied electric load and

$$\tilde{u}_i = u_i C_0/L_1 q_0, \qquad \tilde{\sigma}_{ij} = \sigma_{ij}/q_0$$

$$\tilde{D}_i = D_i C_0/e_0 q_0, \qquad \tilde{\phi} = \phi e_0/L_1 q_0$$

for the applied mechanical load. Here, $C_0 = 21.1$ GPa and $e_0 = 12.322$ Cm^{-2} are representative values of the elastic and piezoelectric moduli, respectively, for the PZT-5A. The shear correction coefficient $\mathcal{K}$ is set equal to $\frac{5}{6}$, although this value was proposed by Reissner for a homogeneous elastic plate. In the FSDT solution, the transverse shear stresses σ_{13} and σ_{23} and the transverse normal stress σ_{33} are obtained by the integration of the equilibrium equations in the thickness direction. The FSDT solution for the electric load is compared with the exact solution in Fig. 2 for length-to-thickness ratios S, ranging from 2 to 40. The FSDT and the exact solution for the axial displacement u_1, the longitudinal stress σ_{11}, and the transverse shear stress σ_{13} are in good agreement even for thick plates with $S < 10$, whereas the transverse deflection u_3 predicted by the FSDT is accurate only for thin plates with $S > 15$. In contrast, if the plate is subjected to the mechanical load, the axial displacement u_1 and the stresses σ_{11} and σ_{13} given by the FSDT are accurate only for thin plates, whereas the transverse deflection u_3 is in excellent agreement with the exact solution for thick plates also, as shown in Fig. 3.

The through-the-thickness variation of the stresses for a thick plate with length-to-thickness ratio $S = 4$ is depicted in Fig. 4 for electrical and mechanical loads. The FSDT gives an affine variation of the longitudinal stress σ_{11} and a parabolic variation for the transverse shear stress σ_{13}, which are in good agreement with the shapes obtained from the exact solution. When the plate is subjected to the electric load, the FSDT predicts the transverse normal stress $\hat{\sigma}_{33}$ to be zero, whereas the exact solution gives a nonzero but small value (Fig. 4c). For the mechanical load, the FSDT gives a cubic through-the-thickness variation for $\tilde{\sigma}_{33}$, which is in excellent agreement with the exact solution as shown in Fig. 4f. The through-the-thickness variations of the longitudinal stress and the transverse shear stress obtained from the FSDT solution agree very well with those computed from the analytical solution of the problem.
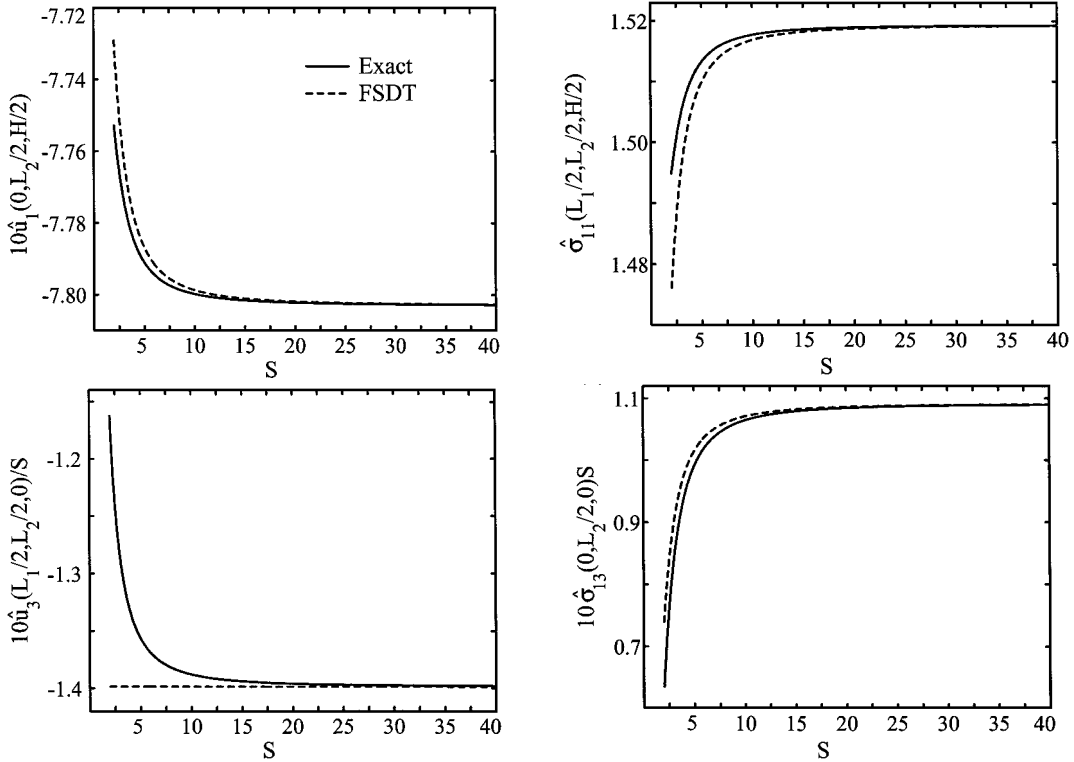
Fig. 2   Axial displacement, transverse deflection, longitudinal stress, and transverse shear stress for an axially poled homogeneous PZT-5A plate subjected to an electric load vs length-to-thickness ratio S.
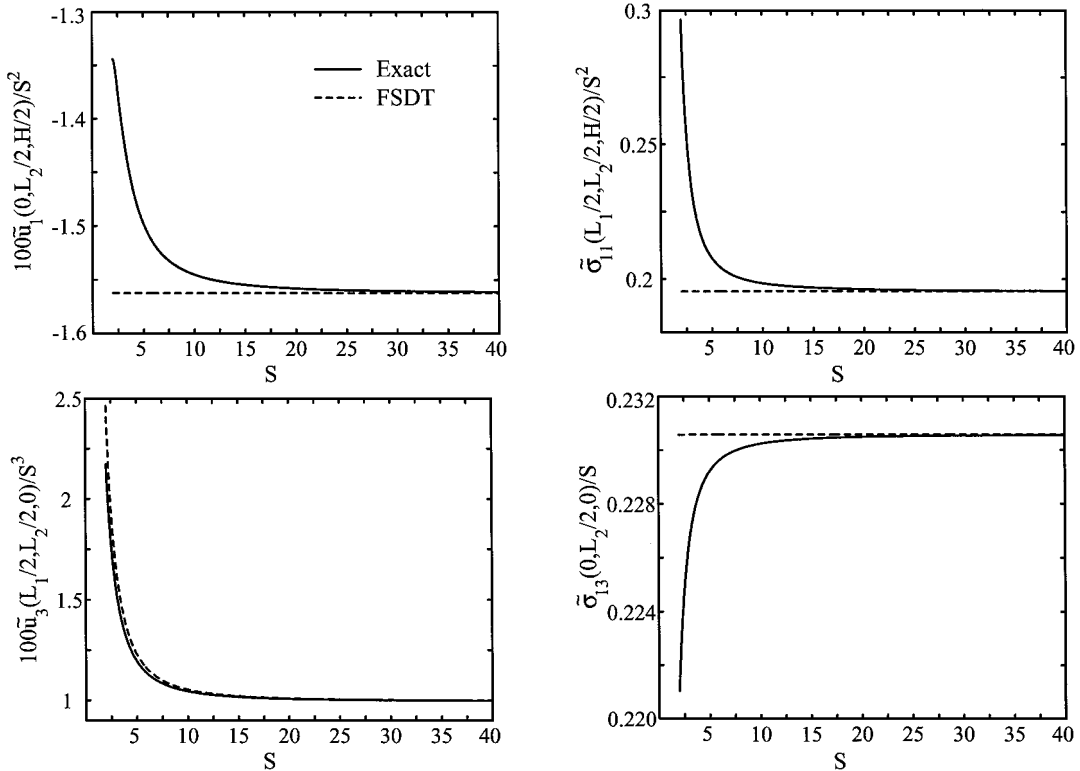

Fig. 3   Axial displacement, transverse deflection, longitudinal stress, and transverse shear stress for an axially poled homogeneous PZT-5A plate subjected to a mechanical load vs length-to-thickness ratio S.

B.   Sandwich Plate with a Piezoelectric Core

We consider a square sandwich plate consisting of an axially poled PZT-5A sandwiched between two graphite–epoxy elastic facing sheets, as shown in Fig 5a. Application of electric potentials $-\phi_0 \cos \pi x_1/L_1 \sin \pi x_2/L_2$ and $\phi_0 \cos \pi x_1/L_1 \sin \pi x_2/L_2$ to the top and bottom surfaces, respectively, of the piezoelectric core will produce a transverse shear deformation in it, thus causing the sandwich structure to deflect in the transverse direction. Only results

from the exact solution are presented in this section. The through-the-thickness variation of the in-plane displacements and stresses for length-to-thickness ratios $S = 4$ and 40 are depicted in Fig. 6. The axial displacement u_1 exhibits a zigzag variation for both thick and thin laminates (Fig 6a). This implies that any equivalent single layer theory, such as the FSDT, that assumes an affine variation of the in-plane displacements through the entire thickness of the laminate will give poor results even for thin sandwich plates. If the
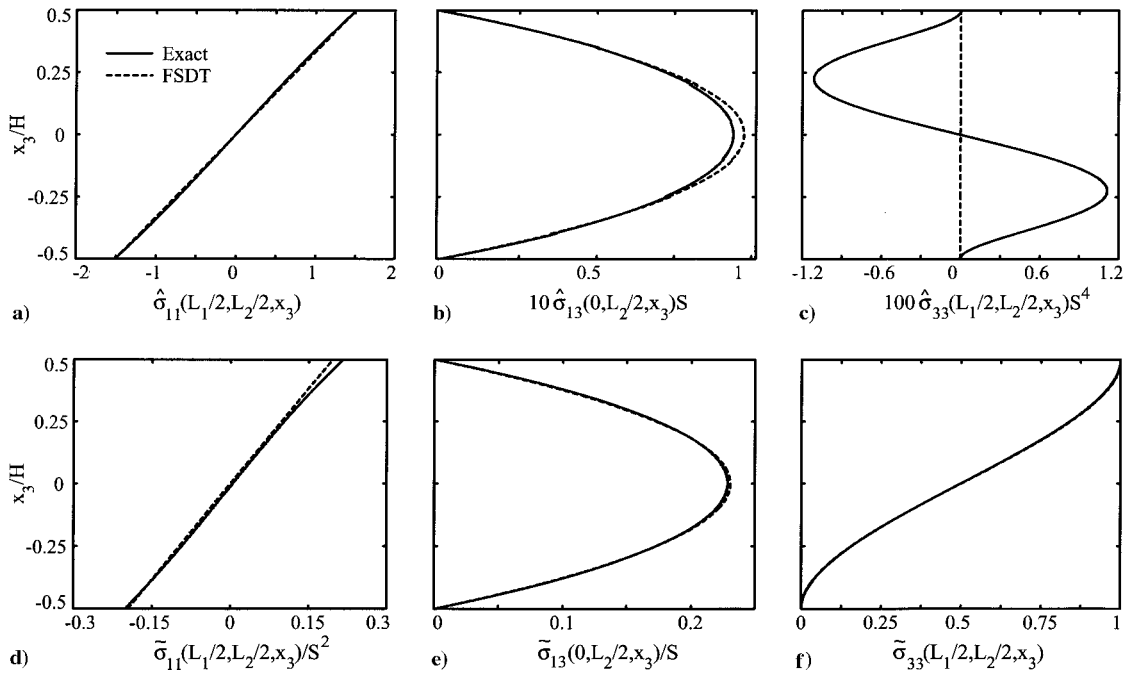
Fig. 4 Through-the-thickness variation of the stresses for an axially poled homogeneous PZT-5A thick plate with $S = 4$: a), b), and c) electrical load; and d), e), and f) mechanical load.
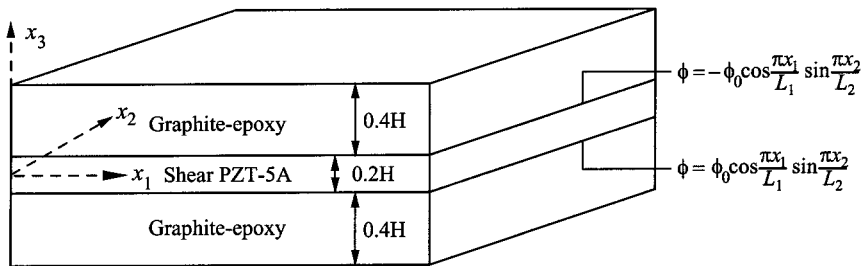

Fig. 5a Axially poled piezoelectric shear actuator core sandwiched between graphite–epoxy facing sheets.
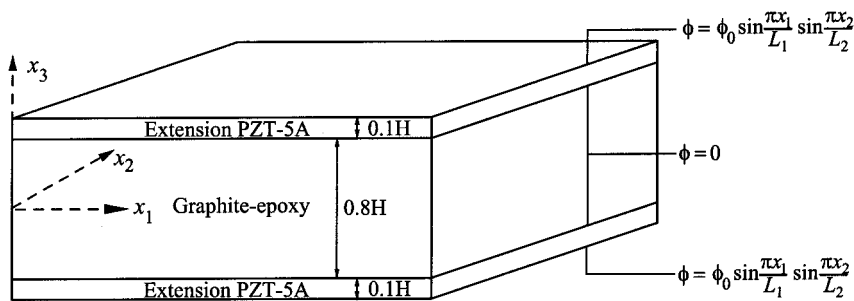

Fig. 5b Corresponding extension actuation configuration with transversely poled actuators.

sandwich plate contains an axially poled piezoelectric core, then a layerwise theory capable of capturing this zigzag behavior must be employed. Zhang and Sun[20,21] have developed a layerwise theory for such sandwich beams by treating the top and bottom elastic sheets as Euler–Bernoulli beams and the axially poled piezoelectric core as a shear deformable Timoshenko beam.

The in-plane displacement u_2 approaches an affine variation through the entire thickness of the sandwich plate for $S = 40$. The longitudinal stress σ_{11} is piecewise affine, and it is significantly smaller in the piezoelectric core than that in the graphite-epoxy facing sheets (Fig. 6c). The longitudinal stress σ_{22} is an order of magnitude smaller than σ_{11}, and it is also piecewise affine. The

transverse shear stress σ_{13} attains its maximum value on the top and bottom surfaces of the piezoelectric core (Fig. 6e). In comparison, the transverse shear stress σ_{23} attains its maximum value on the midsurface of the piezoelectric core as shown in Fig. 6f.

Figure 7 depicts the displacements and stresses in the sandwich structure subjected to the sinusoidal mechanical load $\sigma_{3i}(x_1, x_2, H/2) = q_0 \delta_{3i} \sin(\pi x_1/L_1) \sin(\pi x_2/L_2)$ on its top surface. In this case, the through-the-thickness variation of the axial displacement u_1 approaches an affine distribution through the entire thickness of the plate for increasing length-to-thickness ratios (Fig. 7a), unlike the zigzag variation for the electric load. As expected, the longitudinal stress σ_{11} in the piezoelectric core is smaller
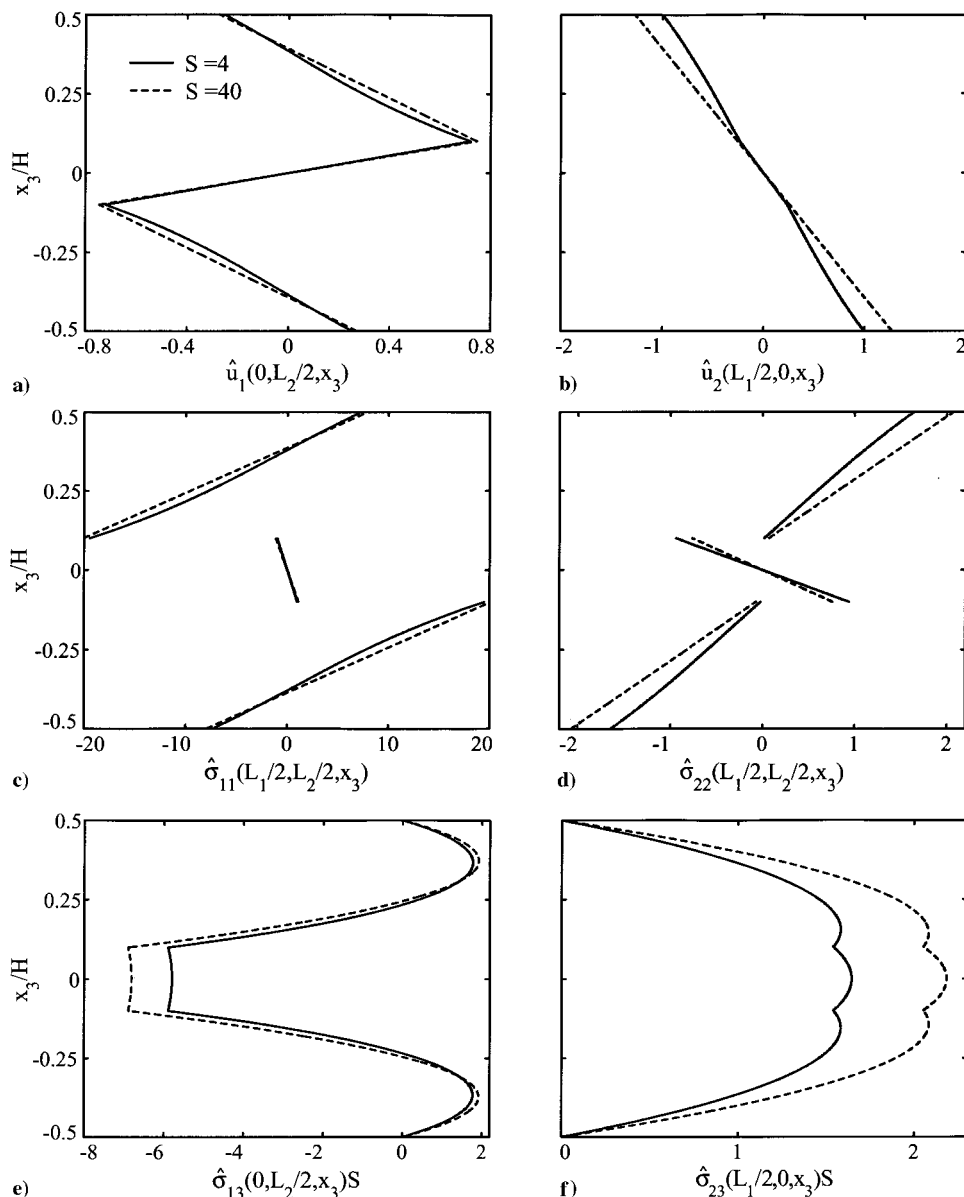
Fig. 6   Through-the-thickness variation of displacements and stresses for the sandwich structure with a piezoelectric shear actuator core between graphite–epoxy facing sheets and subjected to an electric load, $L_1 = L_2$.

than that in the graphite–epoxy facing sheets (Fig. 7b) because the core is closer to the midsurface of the plate. The through-the-thickness variations of the transverse shear stresses σ_{13} and σ_{23} are depicted in Figs. 7c and 7d.

Zhang and Sun[20] studied a cantilever beam made of a piezoelectric shear actuator core sandwiched between two elastic facing sheets, similar to that shown in Fig. 5a, and compared the results with a cantilever beam made of an elastic substrate with piezoelectric extension actuators bonded to its surfaces, like that shown in Fig. 5b. They observed that the greatest advantage provided by the sandwich structure with a piezoelectric shear actuator core is that the longitudinal stresses in the piezoelectric layer are significantly smaller than those observed in the piezoelectric extension actuators. Because we have obtained an exact solution for a sandwich plate with piezoelectric shear actuator core, and the exact solution for a plate with extension actuators was given by Heyliger,[11] we can compare the exact stresses induced in the piezoelectric layer for the two configurations when the edges are simply supported. The material properties for the PZT-5A extension actuators shown in Fig. 5b, poled in the thickness direction, are given by Vel and Batra.[17] The thickness of the piezoelectric shear actuator core in Fig. 5a is the same as the combined thicknesses of the piezoelectric extension actuators in Fig. 5b, and the average applied electric

field intensities in the actuators are also the same for both configurations. For $S = 10$, the transverse deflection u_3 of the plate centroid is $8.025 e_0 \phi_0 / C_0$ for the sandwich plate with a shear actuator and $24.30 e_0 \phi_0 / C_0$ for the plate with extension actuators, that is, a larger electric field has to be applied to the PZT-5A shear actuator than that for the PZT-5A extension actuators to achieve the same transverse deflection. Note, however, that this may not be the case for other piezoelectric actuators because the transverse deflection depends primarily on e_{31} for extension actuators and e_{35} for shear actuators. Therefore, the relative magnitudes of these two coefficients for the piezoelectric material will determine which of the two configurations has a larger deflection for the same applied electric field intensity.

The maximum longitudinal stress in the piezoelectric actuator divided by the centroidal deflection of the sandwich plate is plotted against the length-to-thickness ratio S in Fig. 8a. The stresses are compared at different thickness locations for the two configurations because the maximum longitudinal stress σ_{11} in the piezoelectric shear actuator occurs at $x_3 = 0.1 H^-$ (and $-0.1 H^+$), and it occurs at $x_3 = 0.4 H^+$ (and $-0.4 H^-$) for the piezoelectric extension actuators. We use $H^{\pm}$, defined as $\lim_{\delta \to 0} H \pm \delta$, because the longitudinal stress may be discontinuous at the interface between laminae. As is evident, the maximum longitudinal stress σ_{11} in the actuator to

Table 2   Mechanical displacements, stresses, electric potential, and electric displacement at specific locations of a square sandwich plate made of an axially poled piezoelectric shear actuator core sandwiched between graphite–epoxy or aluminum facing sheets and subjected to an electric load

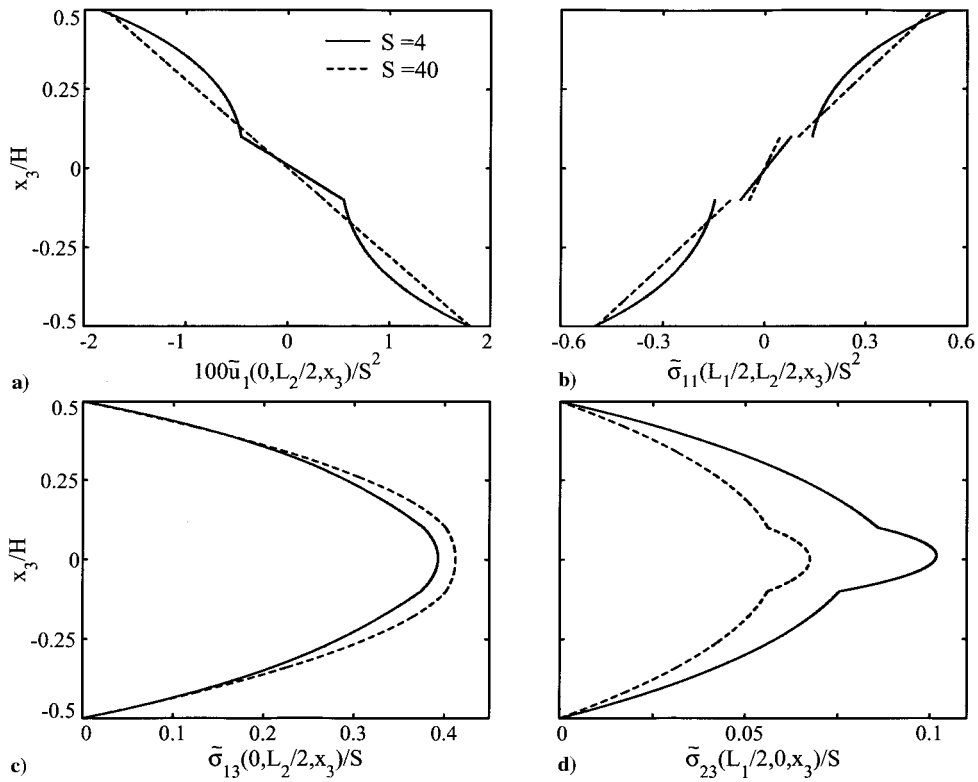| Variable	Graphite–epoxy facing sheets			Aluminum facing sheets		
	$S = 4$	$S = 10$	$S = 40$	$S = 4$	$S = 10$	$S = 40$
$\hat{u}_1(0, L_2/2, 0.1H)$	0.7209	0.7412	0.7451	0.8193	0.8482	0.8540
$\hat{u}_2(L_1/2, 0, 0.5H)$	−0.9959	−1.2179	−1.2697	−0.6513	−0.7147	−0.7274
$\hat{u}_3(L_1/2, L_2/2, 0)/S$	0.7711	0.8025	0.8101	0.4483	0.4611	0.4635
$\hat{\sigma}_{11}(L_1/2, L_2/2, 0.5H)$	7.3066	7.8470	7.9416	0.1849	−0.1656	−0.2386
$\hat{\sigma}_{22}(L_1/2, L_2/2, 0.5H)$	1.6436	1.9926	2.0736	6.8808	7.4231	7.5312
$\hat{\sigma}_{12}(L_1/4, L_2/4, 0.5H)$	−0.6672	−0.7944	−0.8235	−0.8602	−0.8836	−0.8879
$\hat{\sigma}_{13}(L_1/4, L_2/2, 0)S$	−4.0986	−4.6885	−4.8169	−4.5061	−4.8791	−4.9537
$\hat{\sigma}_{23}(L_1/2, L_2/4, 0)S$	1.1635	1.4715	1.5445	1.6252	1.9132	1.9722
$\hat{\sigma}_{33}(L_1/2, L_2/2, 0.3H)S^2$	−1.3004	−1.4644	−1.4980	−1.1876	−1.2233	−1.2299
$\hat{\phi}(L_1/2, L_2/2, 0.05H)$	−0.4992	−0.4999	−0.5000	−0.4993	−0.4999	−0.5000
$\hat{D}_1(L_1/2, L_2/2, 0.1H)$	−10.4195	−10.5393	−10.5632	−10.803	−10.9627	−10.9941
$\hat{D}_2(L_1/4, L_2/4, 0.1H)$	4.1060	4.1110	4.1107	4.4265	4.4487	4.4528
$\hat{D}_3(L_1/4, L_2/2, 0)/S$	21.8052	22.0518	22.1024	21.7817	22.0502	22.1023

Fig. 7   Through-the-thickness variation of displacements and stresses for the sandwich structure with a piezoelectric shear actuator core between graphite–epoxy facing sheets and subjected to a mechanical load, $L_1 = L_2$.

achieve a given transverse deflection of the plate is significantly smaller for shear actuators than for extension actuators. Therefore, it is advantageous to use shear actuators instead of extension actuators because a large longitudinal stress is detrimental to the brittle piezoceramic material. Thus, our comparison of the exact longitudinal stresses for the two configurations supports the conclusion of Zhang and Sun.[20] The transverse shear stress σ_{13} in the piezoelectric layer is maximum on the interface $x_3 = 0.1H$ between it and the graphite–epoxy layer for the shear actuation configuration and at $x_3 = 0.4H$ for the extension actuation configuration. A comparison of the maximum σ_{13} divided by the midpoint deflection is shown in Fig. 8b for various length-to-thickness ratios. It reveals that the maximum transverse shear stress is only slightly larger for shear actuators than that for extension actuators. However, the maximum shear stress σ_{13} is significantly smaller than the maximum longitudinal stress σ_{11} in the extension actuators, and, therefore, the overall stress level within the shear actuator is still smaller than that in the extension actuator. Note that Heyliger[11] has considered electrically grounded edges at $x_1 = 0$ and L_1 and a sinusoidal electric load in the

x_1 direction for extension actuators, whereas we have assumed the edges $x_1 = 0$ and L_1 to be electrically insulated and have assumed a cosinusoidal electric load in the x_1 direction to obtain exact solutions for shear actuators. In spite of these differences, the results presented in this section provide a useful comparison of the effectiveness of extension and shear actuators.

Numerical results at specific points of the square sandwich plate with a PZT-5A shear actuator core and having either graphite–epoxy or aluminum facing sheets are given in Table 2 for the electric load. Young's modulus and Poisson's ratio for aluminum are assumed to be 70.3 GPa and 0.345, respectively.[20]

In all of the preceding problems studied, the piezoelectric layers extended over the entire length of the laminate. However, in practice, small patches of a piezoelectric material are either affixed to the surfaces of a structure or embedded in it. Analytical solutions for the cylindrical bending of laminates with segmented sensors and/or actuators have been obtained by Vel and Batra[16] by using the Eshelby–Stroh formalism. The equilibrium equations are exactly satisfied at every point in the body, and the boundary conditions

a) Longitudinal stress
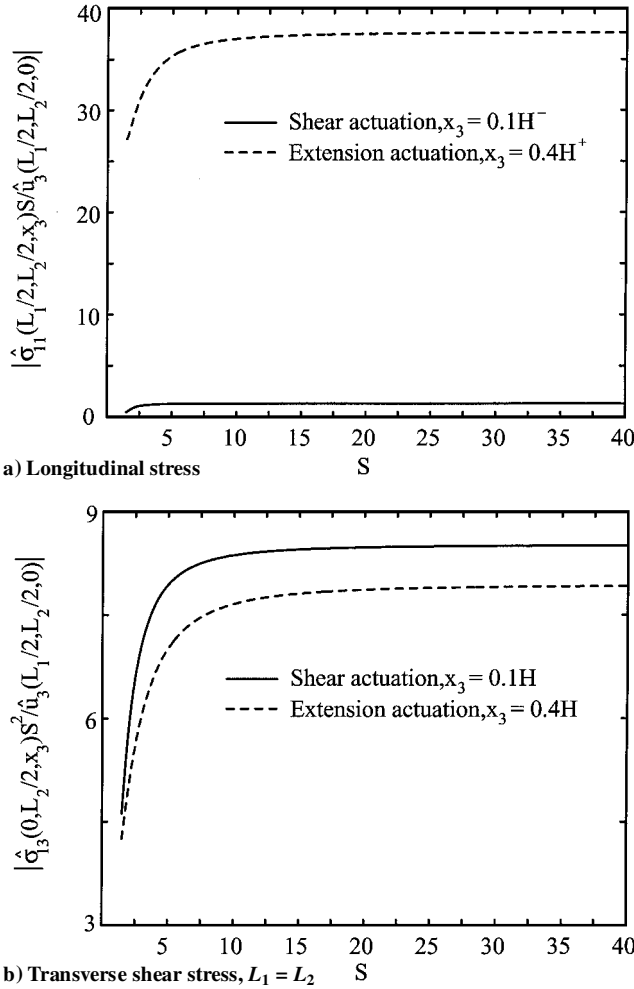

b) Transverse shear stress, $L_1 = L_2$

Fig. 8 Comparison of the stresses in the piezoelectric layer for the shear actuation mechanism and the corresponding extension actuation mechanism for an electric load.

and the continuity conditions at the interfaces are satisfied in the sense of Fourier series. For the problems studied herein with simply supported edges, both the equilibrium equations and boundary conditions are satisfied pointwise.

VI. Conclusions

We have obtained an exact solution for the three-dimensional static deformations of simply supported laminated thick plates with embedded piezoelectric shear actuators. The governing equations of linear piezoelectricity, the boundary conditions at the simply supported edges, and the interface conditions between dissimilar layers are exactly satisfied. We have developed a plate theory, based on the displacement field of the FSDT, for homogeneous axially poled piezoelectric plates with a known variation of the electric potential field. For a square plate, all of the displacements and stresses obtained by using the FSDT are in good agreement with the exact solution when the length-to-thickness ratio is greater than 15. The deviation between the two sets of results increases as the length-to-thickness ratio decreases.

We have also analyzed deformations of a sandwich plate with an axially polarized piezoelectric core sandwiched between two elastic surface layers. The application of an electric field in the thickness direction induces transverse shear deformation of the core, thus generating the desired transverse deflection. The through-thickness variation of the axial displacement takes a zigzag shape for both thick and thin laminates. Thus, an equivalent single layer theory, like the FSDT, that assumes a linear variation of the axial displacement through the entire thickness of the laminate should not be used to analyze such structures, even when the thickness of the plate is small when compared to its length. Instead, a layerwise theory ought to be employed for all sandwich laminates.

A comparison of stresses in a sandwich laminate with those in an equivalent surface-mounted extension actuator configuration reveals that the longitudinal stresses within the shear actuators are significantly smaller than those in the extension actuators. Thus, it is advantageous to use shear actuators because large longitudinal stresses can be detrimental to the brittle piezoceramic material.

The results presented herein should help others validate simpler models for sandwich structures with shear actuators.

Appendix: Solution for R_k

The solution for R_k in terms of the applied electric potential, geometric, and material parameters of the homogeneous rectangular simply supported plate is

$$R_1 = 0$$

$$
\begin{aligned}
R_2 = & \Big[2S\phi_0 \Big(-A^2 \big[\pi^2 P_{11} Q_{22} + 12S^2 \mathcal{K} P_{35} \big(A^2 Q_{12} + Q_{22} \big) \big] Q_{44} \\
& - A^4 P_{11} \big(\pi^2 Q_{22} + 12A^2 S^2 \mathcal{K} Q_{44} \big) Q_{55} + P_{26} \big\{ \pi^2 \big(A^2 Q_{12} \\
& - Q_{22} \big) Q_{44} + A^2 \big[\pi^2 \big(A^2 Q_{12} - Q_{22} \big) - 24 A^2 S^2 \mathcal{K} Q_{44} \big] Q_{55} \big\} \\
& - A^4 \big[24 S^2 \mathcal{K} P_{35} Q_{44} + \pi^2 P_{11} \big(Q_{44} + A^2 Q_{55} \big) \big] Q_{66} \\
& + A^2 P_{12} \big[-12 A^2 S^2 \mathcal{K} Q_{44} Q_{55} + \pi^2 Q_{12} \big(Q_{44} + A^2 Q_{55} \big) \\
& + \pi^2 \big(Q_{44} + A^2 Q_{55} \big) Q_{66} \big] \Big) \Big] \Big/ \Big[L_1 \Big(A^2 \big\{ -\pi^2 \big(Q_{12}^2 - Q_{11} Q_{22} \big) Q_{44} \\
& + \big[-A^2 \pi^2 \big(Q_{12}^2 - Q_{11} Q_{22} \big) + 12 S^2 \mathcal{K} \big(A^4 Q_{11} + 2A^2 Q_{12} \\
& + Q_{22} \big) Q_{44} \big] Q_{55} \big\} + \big\{ \pi^2 \big(A^4 Q_{11} - 2A^2 Q_{12} + Q_{22} \big) Q_{44} \\
& + A^2 \big[\pi^2 \big(A^4 Q_{11} - 2A^2 Q_{12} + Q_{22} \big) + 48 A^2 S^2 \mathcal{K} Q_{44} \big] Q_{55} \big\} Q_{66} \Big) \Big]
\end{aligned}
$$

$$R_3 = 0$$

$$
\begin{aligned}
R_4 = & \Big[2AS\phi_0 \Big(P_{26} \big\{ -\pi^2 \big(A^2 Q_{11} - Q_{12} \big) Q_{44} - A^2 \big(\pi^2 \big[A^2 Q_{11} \\
& - Q_{12} \big) + 24 S^2 \mathcal{K} Q_{44} \big] Q_{55} \big\} + P_{12} \big\{ -A^2 \big[12 S^2 \mathcal{K} Q_{44} Q_{55} \\
& + \pi^2 Q_{11} \big(Q_{44} + A^2 Q_{55} \big) \big] - \pi^2 \big(Q_{44} + A^2 Q_{55} \big) Q_{66} \big\} \\
& + A^2 \big\{ 12 A^2 S^2 \mathcal{K} P_{35} Q_{11} Q_{44} + \pi^2 P_{11} Q_{12} Q_{44} \\
& + 12 S^2 \mathcal{K} P_{35} Q_{12} Q_{44} + A^2 \pi^2 P_{11} Q_{12} Q_{55} \\
& - 12 A^2 S^2 \mathcal{K} P_{11} Q_{44} Q_{55} \\
& + \big[24 S^2 \mathcal{K} P_{35} Q_{44} + \pi^2 P_{11} \big(Q_{44} + A^2 Q_{55} \big) \big] Q_{66} \big\} \Big) \Big] \Big/ \\
& \Big[L_1 \Big(A^2 \big\{ -\pi^2 \big(Q_{12}^2 - Q_{11} Q_{22} \big) Q_{44} + \big[-A^2 \pi^2 \big(Q_{12}^2 \\
& - Q_{11} Q_{22} \big) + 12 S^2 \mathcal{K} \big(A^4 Q_{11} + 2A^2 Q_{12} + Q_{22} \big) Q_{44} \big] Q_{55} \big\} \\
& + \big\{ \pi^2 \big(A^4 Q_{11} - 2A^2 Q_{12} + Q_{22} \big) Q_{44} + A^2 \big[\pi^2 \big(A^4 Q_{11} \\
& - 2A^2 Q_{12} + Q_{22} \big) + 48 A^2 S^2 \mathcal{K} Q_{44} \big] Q_{55} \big\} Q_{66} \Big) \Big]
\end{aligned}
$$

$$
\begin{aligned}
R_5 = & \Big[2A^2 S\phi_0 \Big(A^2 \pi^2 P_{12} Q_{11} Q_{44} + A^2 \pi^2 P_{26} Q_{11} Q_{44} \\
& - A^2 \pi^2 P_{11} Q_{12} Q_{44} - \pi^2 P_{26} Q_{12} Q_{44} - A^2 \pi^2 P_{12} Q_{12} Q_{55} \\
& - A^2 \pi^2 P_{26} Q_{12} Q_{55} + A^2 \pi^2 P_{11} Q_{22} Q_{55} + \pi^2 P_{26} Q_{22} Q_{55} \\
& + 12 A^4 S^2 \mathcal{K} P_{11} Q_{44} Q_{55} + 12 A^2 S^2 \mathcal{K} P_{12} Q_{44} Q_{55} \\
& + 24 A^2 S^2 \mathcal{K} P_{26} Q_{44} Q_{55} + \pi^2 \big(-A^2 P_{11} + P_{12} \big) \big(Q_{44} \\
& - A^2 Q_{55} \big) Q_{66} + P_{35} \big\{ A^2 \big(\pi^2 \big(Q_{12}^2 - Q_{11} Q_{22} \big) - 12 S^2 \mathcal{K} \\
& \times \big(A^2 Q_{11} + Q_{12} \big) Q_{44} - \big[\pi^2 \big(A^4 Q_{11} - 2A^2 Q_{12} + Q_{22} \big) \\
& + 24 A^2 S^2 \mathcal{K} Q_{44} \big] Q_{66} \big\} \Big) \Big] \Big/ \Big(A^2 \pi \big\{ -\pi^2 \big(Q_{12}^2 - Q_{11} Q_{22} \big) Q_{44} \\
& + \big[-A^2 \pi^2 \big(Q_{12}^2 - Q_{11} Q_{22} \big) + 12 S^2 \mathcal{K} \big(A^4 Q_{11} + 2A^2 Q_{12} \\
& + Q_{22} \big) Q_{44} \big] Q_{55} \big\} + \pi \big\{ \pi^2 \big(A^4 Q_{11} - 2A^2 Q_{12} + Q_{22} \big) Q_{44} \\
& + A^2 \big[\pi^2 \big(A^4 Q_{11} - 2A^2 Q_{12} + Q_{22} \big) + 48 A^2 S^2 \mathcal{K} Q_{44} \big] Q_{55} \big\} Q_{66} \Big)
\end{aligned}
$$

where $A = L_2/L_1$ is the aspect ratio of the plate and $S = L_1/H$ is the length-to-thickness ratio.

References

[1]Crawley, E. F., and de Luis, J., "Use of Piezoelectric Actuators as Elements of Intelligent Structures," *AIAA Journal*, Vol. 25, No. 10, 1987, pp. 1373–1385.

[2]Crawley, E. F., and Anderson, E. H., "Detailed Models of Piezoceramic Actuation of Beams," *Journal of Intelligent Material Systems and Structures*, Vol. 1, No. 1, 1990, pp. 4–25.

[3]Lee, C. K., "Theory of Laminated Piezoelectric Plates for the Design of Distributed Sensors/Actuators. Part 1: Governing Equations and Reciprocal Relationships," *Journal of the Acoustical Society of America*, Vol. 87, No. 3, 1990, pp. 1144–1158.

[4]Huang, J. H., and Wu, T. L., "Analysis of Hybrid Multilayered Piezoelectric Plates," *International Journal of Engineering Science*, Vol. 34, No. 2, 1996, pp. 171–181.

[5]Mitchell, J. A., and Reddy, J. N., "A Refined Hybrid Plate Theory for Composite Laminates with Piezoelectric Laminae," *International Journal of Solids and Structures*, Vol. 32, No. 16, 1995, pp. 2345–2367.

[6]Robbins, D. H., and Reddy, J. N., "Analysis of Piezoelectrically Actuated Beams Using a Layer-Wise Displacement Theory," *Computers and Structures*, Vol. 41, No. 2, 1991, pp. 265–279.

[7]Batra, R. C., and Liang, X. Q., "Finite Dynamic Deformations of Smart Structures," *Computational Mechanics*, Vol. 20, No. 5, 1997, pp. 427–438.

[8]Ray, M. C., Rao, K. M., and Samanta, B., "Exact Solution for Static Analysis of Intelligent Structures Under Cylindrical Bending," *Computers and Structures*, Vol. 47, No. 6, 1993, pp. 1031–1042.

[9]Heyliger, P., and Brooks, S., "Exact Solutions for Laminated Piezoelectric Plates in Cylindrical Bending," *Journal of Applied Mechanics*, Vol. 63, No. 4, 1996, pp. 903–910.

[10]Heyliger, P., "Static Behavior of Laminated Elastic/Piezoelectric Plates," *AIAA Journal*, Vol. 32, No. 12, 1994, pp. 2481–2484.

[11]Heyliger, P., "Exact Solutions for Simply Supported Laminated Piezoelectric Plates," *Journal of Applied Mechanics*, Vol. 64, No. 2, 1997, pp. 299–306.

[12]Bisegna, P., and Maceri, F., "An Exact Three-Dimensional Solution for Simply Supported Rectangular Piezoelectric Plates," *Journal of Applied Mechanics*, Vol. 63, No. 3, 1996, pp. 628–638.

[13]Lee, J. S., and Jiang, L. Z., "Exact Electroelastic Analysis of Piezoelectric Laminae via State Space Approach," *International Journal of Solids and Structures*, Vol. 33, No. 7, 1996, pp. 977–990.

[14]Yang, J. S., Batra, R. C., and Liang, X. Q., "The Cylindrical Bending Vibration of a Laminated Elastic Plate due to Piezoelectric Actuators," *Smart Materials and Structures*, Vol. 3, No. 4, 1994, pp. 485–493.

[15]Batra, R. C., Liang, X. Q., and Yang, J. S., "The Vibration of a Simply Supported Rectangular Elastic Plate due to Piezoelectric Actuators," *International Journal of Solids and Structures*, Vol. 33, No. 11, 1996, pp. 1597–1618.

[16]Vel, S. S., and Batra, R. C., "Cylindrical Bending of Laminated Plates with Distributed and Segmented Piezoelectric Actuators/Sensors," *AIAA Journal*, Vol. 38, No. 5, 2000, pp. 857–867.

[17]Vel, S. S., and Batra, R. C., "Three-Dimensional Analytical Solution for Hybrid Multilayered Piezoelectric Plates," *Journal of Applied Mechanics*, Vol. 67, No. 3, 2000, pp. 558–567.

[18]Sun, C. T., and Zhang, X. D., "Use of Thickness-Shear Mode in Adaptive Sandwich Structures," *Smart Materials and Structures*, Vol. 4, No. 3, 1995, pp. 202–206.

[19]"Data for Designers," Electro Ceramic Div., Morgan Matroc, Bedford, OH.

[20]Zhang, X. D., and Sun, C. T., "Formulation of an Adaptive Sandwich Beam," *Smart Materials and Structures*, Vol. 5, No. 6, 1996, pp. 814–823.

[21]Zhang, X. D., and Sun, C. T., "Analysis of a Sandwich Plate Containing a Piezoelectric Core," *Smart Materials and Structures*, Vol. 8, No. 1, 1999, pp. 31–40.

[22]Benjeddou, A., Trindade, M. A., and Ohayon, R., "A Unified Beam Finite Element Model for Extension and Shear Piezoelectric Actuation Mechanisms," *Journal of Intelligent Material Systems and Structures*, Vol. 8, No. 12, 1997, pp. 1012–1025.

[23]Vidoli, S., and Batra, R. C., "Derivation of Plate and Rod Equations for a Piezoelectric Body from a Mixed Three-Dimensional Variational Principle," *Journal of Elasticity*, Vol. 59, Nos. 1/3, 2000, pp. 23–50.

[24]Vel, S. S., and Batra, R. C., "Analysis of Piezoelectric Bimorphs and Plates with Segmented Actuators," *Thin-Walled Structures*, Vol. 38, No. 1, 2001, pp. 23–44.

[25]Vel, S. S., and Batra, R. C., "Exact Solution for the Cylindrical Bending of Laminated Plates with Embedded Shear Actuators," *Smart Materials and Structures* (to be published).

[26]Tiersten, H. F., *Linear Piezoelectric Plate Vibrations*, Plenum, New York, 1969.

[27]Fan, J., and Ye, J., "An Exact Solution for the Statics and Dynamics of Laminated Thick Plates with Orthotropic Layers," *International Journal of Solids and Structures*, Vol. 26, No. 5–6, 1990, pp. 655–662.

[28]Tang, Y. Y., Noor, A. K., and Xu, K., "Assessment of Computational Models for Thermoelectroelastic Multilayered Plates," *Computers and Structures*, Vol. 61, No. 5, 1996, pp. 915–933.

A. N. Palazotto
Associate Editor